Anisotropic Pedestrian Evacuation Modeling: Pedestrian Travel-Time Maps for Alaska Coastal Communities

by

A.E. Macpherson[1], D.J. Nicolsky[1], and R.D. Koehler[2]

ABSTRACT

Alaska coastal communities are threatened by tsunamis that could reach the coast within minutes after an earthquake. Pedestrian evacuation from tsunamis is evaluated using an anisotropic modeling approach developed by the United States Geological Survey (USGS). The applied method is based on path-distance algorithms and accounts for variations in land cover and directionality in slope. The developed pedestrian travel-time maps are community specific and are computed for the worst-case hypothetical tsunami scenario in each community. At least four different scenarios of pedestrian evacuation to safety are considered. Results presented here are intended to provide guidance to local emergency management agencies in tsunami inundation assessment, evacuation planning, and public education to mitigate future tsunami hazards.

[1] *Alaska Earthquake Center, Geophysical Institute, University of Alaska, P.O. Box 757320, Fairbanks, Alaska 99775-7320; djnicolsky@alaska.edu*

[2] *Department of Natural Resources, Division of Geological & Geophysical Surveys (DGGS), 3354 College Road, Fairbanks, AK 99709; richard.koehler@alaska.gov; R.D. Koehler now at Nevada Bureau of Mines and Geology, Mackay School of Earth Science and Engineering, University of Nevada, Reno, 1664 North Virginia St, MS 178, Reno, NV 89557*

INTRODUCTION

Subduction of the Pacific plate under the North American plate has resulted in numerous great earthquakes and has the highest potential to generate tsunamis in Alaska (Dunbar and Weaver, 2008). The Alaska–Aleutian subduction zone (figure 1), the fault formed by the Pacific–North American plate interface, is the most seismically active tsunamigenic fault zone in the U.S. The latest sequence of great earthquakes along the Alaska–Aleutian subduction zone began in 1938 with a M_w 8.3 earthquake west of Kodiak Island (Estabrook and others, 1994). Four subsequent events, the 1946 M_w 8.6 Aleutian (Lopez and Okal, 2006), the 1957 M_w 8.6 Andreanof Island (Johnson and Satake, 1993), the 1964 M_w 9.2 Great Alaska (Kanamori, 1970), and the 1965 M_w 8.7 Rat Island (Wu and Kanamori, 1973) earthquakes, ruptured almost the entire length of the subduction zone. Tsunamis generated by these great earthquakes reached Alaska coastal communities within minutes after the earthquakes and resulted in widespread damage and loss of life (National Geophysical Database Center/World Data Service [NGDC/WDS]). Saving lives and property depends on how well a community is prepared, which further depends on estimating potential flooding of the coastal zone in the event of a local or distant tsunami.

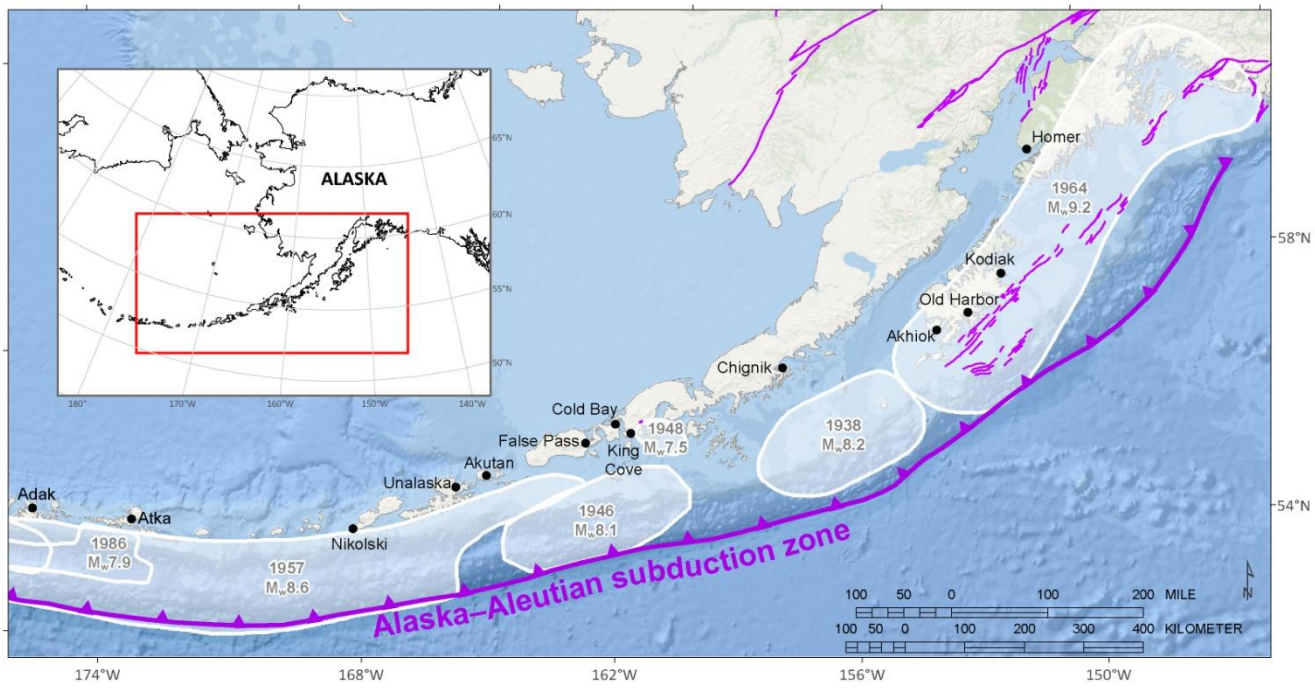

Figure 1: Map of south-central Alaska and the Alaska Peninsula, identifying major active or potentially active faults (dark purple lines) and the rupture zones of the 1938, 1946, 1948, 1957, 1964, and 1965 earthquakes (light shaded areas).

The production of tsunami hazard maps for a community consists of several stages. First we develop hypothetical tsunami scenarios on the basis of credible potential tsunamigenic earthquakes and submarine landslides. Then we perform model simulations for each of these scenarios. The results are compared with any historical tsunami observations, if such data exist. Finally we develop a "worst case" inundation line that encompasses the maximum extent of flooding based on model simulation of all source scenarios and historical observations. The "worst case" inundation line becomes a basis for local tsunami hazard planning and development of pedestrian evacuation maps for the communities. Refer to Suleimani and others (2010, 2013, 2015) and Nicolsky and others (2011, 2013, 2014, 2015) for a detailed discussion of the process.

In this series of reports, we employ the pedestrian evacuation modeling tools developed by USGS (Wood and Schmidtlein, 2012, 2013; Jones and others, 2014) to provide guidance to emergency managers and community planners in assessment of the amount of time required for people to evacuate out of the tsunami-hazard zone. The maps of pedestrian travel time can help to identify areas on which to focus evacuation training and tsunami education. The travel-time maps developed from this method can also be used to examine the potential benefits of vertical evacuation structures, which are buildings or berms designed to provide a local high ground in low-lying areas of the hazard zone. This initial report outlines the methodology and approach that will be applied in subsequent reports for various communities along the Alaska–Aleutian subduction zone.

PEDESTRIAN EVACUATION MODELING METHODOLOGY

Pedestrian evacuation modeling to address population vulnerability to tsunami hazards was successfully applied to coastal communities in Alaska by Wood and Peters (2015). The authors modeled anisotropic pedestrian evacuation in Kodiak, Cordova, Seward, Valdez, and Whittier and assessed variations in population exposure as a function of travel time out of tsunami hazard zones. In this series of reports, we only focus on estimating the pedestrian evacuation times to safety. We do not assess the population exposure because of large and often unpredictable variations in the number of seasonal workers and tourists in the hazard zone.

Pedestrian evacuation potential is modeled using an anisotropic, least-cost distance (LCD) approach using the Pedestrian Evacuation Analyst Extension (PEAE) for ArcGIS (Jones and others, 2014). Following Wood and Peters (2015) we choose an LCD approach over an agent-based approach (such as in Yeh and others, 2009) because we focus on simulating an evacuation time of the population in the hazard zone as a whole. The LCD approach incorporates variations in land cover and the directionality of an evacuation (Wood and Schmidtlein, 2012). Note that the agent-based models rely heavily on information about route capacity, evacuee crowding, and potential choking points when calculating the travel time to safety (Wood and Schmidtlein, 2012). Choking points are largely absent in Alaska communities because of their low population density. If such choking points exist (such as stairs, a narrow path, or gates) it is recommended that the LCD approach be supplemented with an agent-based approach with a specific population distribution.

Finally, we note that the anisotropic, least-cost distance model used (Jones and others, 2014) focuses on the evacuation landscape, using physical characteristics such as elevation, slope, and land cover to calculate the most efficient path to safety. Therefore computed travel times are based on optimal routes; actual travel times may be greater depending on individual route choice and environmental conditions during an evacuation. Data required for pedestrian evacuation modeling include: (1) the tsunami hazard zone, (2) assembly areas, (3) digital elevation model (DEM) of the community, and (4) land-cover datasets. In the remainder of this section, we provide a generic description of the above-mentioned data applicable for all considered coastal communities unless otherwise noted.

The tsunami hazard zones and associated digital elevation models are available from published Alaska Division of Geological & Geophysical Surveys (DGGS) tsunami inundation reports (Suleimani and others, 2010, 2013, 2015; Nicolsky and others, 2011, 2013, 2014, 2015). Existing and considered assembly areas (determined by discussions with local residents or emergency managers and/or published documents) are typically defined as roadways at the boundary of the tsunami hazard zone, and through which a population can evacuate away from the incoming tsunami.

The spatial resolution of the DEM has a large impact on the results of the computed pedestrian travel-time map, as the path distance approach calculates distances and slopes between cells of varying elevations. A model sensitivity analysis showed that coarser-resolution elevation tended to underestimate travel times across the hazard zone (Wood and Schmidtlein, 2012). DEM resolution, in particular, can have critical impacts on the results. For example, if the resolution is too coarse it might not be possible to maintain connectivity on narrow roads or trails when modeling evacuation via roads only. Some variations

to the DEMs are made by increasing or decreasing the cell size of the DEM. The chosen DEM resolution is detailed in individual community reports.

A land-cover layer is created with the 2011 National Land Cover Database (NLCD) for Alaska (Jin and others, 2013) as a starting point. When available, local GIS data sources are utilized for roads, streams, and building footprints. Aerial imagery, filtered by the Best Data Layer (BDL) and available through the Web Mapping Service (WMS) provided by the Geographic Information Network of Alaska (GINA), supplements the NLCD layer and helps with outlining the footprints for buildings, roads, and trails. Generally, up to eight or nine land-cover types are created for each community; however, some areas might have additional or fewer land-cover types. An example of the land-cover types for the community of Homer is shown in figure 2.

Figure 2: The developed land-cover classification for Homer, Alaska. Sources: 2011NLCD, GINA BDL WMS, and site visit notations.

Because global datasets such as NLCD are prone to have some errors, and also because of the potential overgeneralization of the land-cover dataset caused by the large pixel size (30 m [98 ft]), we conduct on-site visits and verify the specified land-cover types for each community studied. The data collected during the community visits allow for finer delineations between land-cover classes and facilitates development of more accurate land-cover polygons. The development of the land-cover layer for a given community is specified in the corresponding report.

PEDESTRIAN EVACUATION MODELING WORKFLOW

A foundation of the PEAE toolkit is a spatial matrix of grid cells—a raster—where each value represents the difficulty, or cost, of movement across a landscape. In this section we describe steps necessary to assemble this spatial matrix and then to compute the pedestrian travel-time map. Before we proceed to the description of the step-by-step procedures, we note that each community has a unique set of scenarios. Namely, for all considered communities we model evacuation according to four scenarios:

Scenario 1. Evacuation to the hazard zone boundary across all terrain

Scenario 2. Evacuation to the hazard zone boundary by roads only

Scenario 3. Evacuation to the nearest assembly area across all terrain

Scenario 4. Evacuation to the nearest assembly area by roads only

The following steps, from Jones and others (2014), are illustrated in the flow chart shown in figure 3. Steps 1–4 are repeated for each scenario considered.

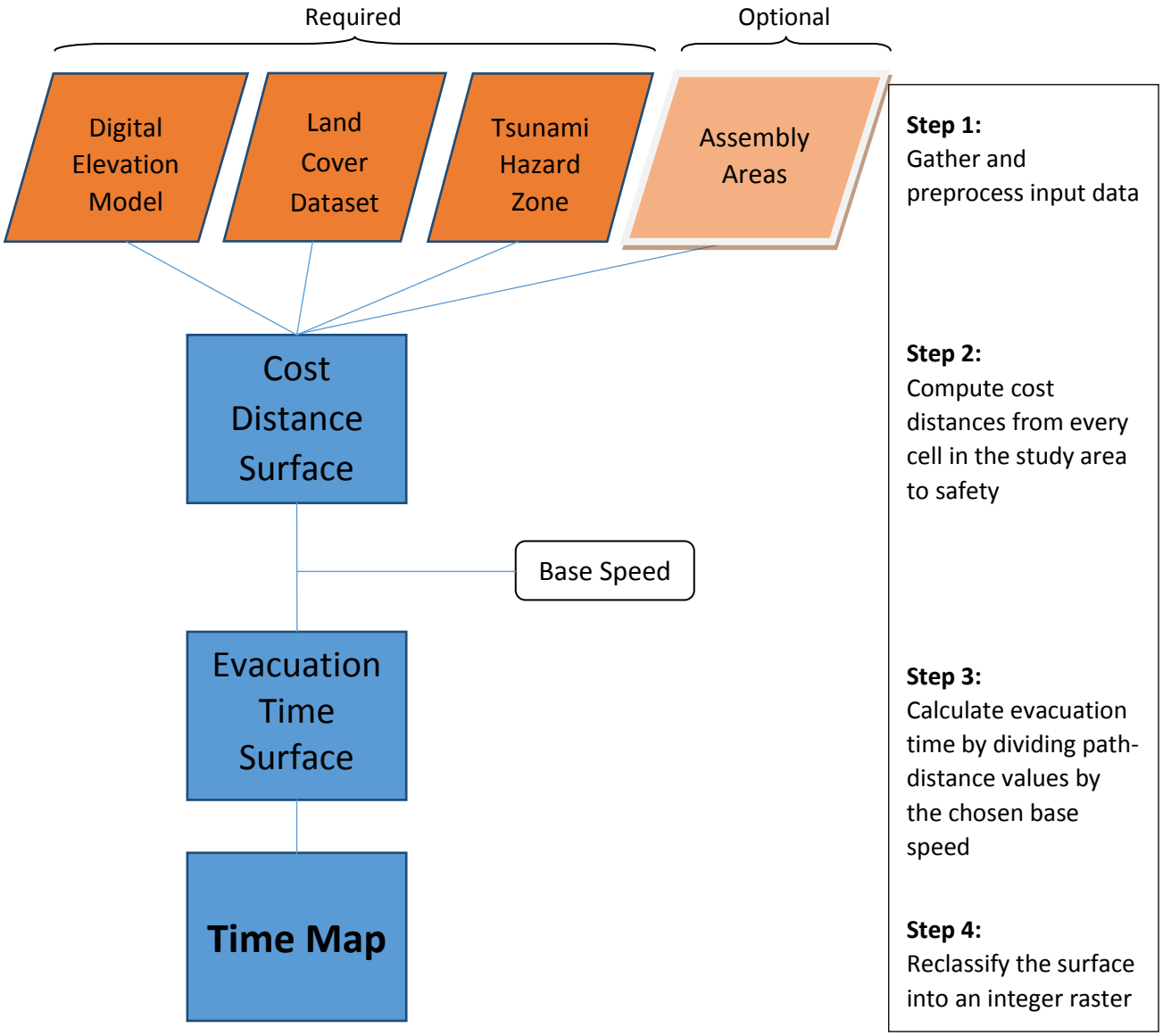

Figure 3: Flow chart of pedestrian evacuation modeling workflow.

Step 1

Once the DEM and land-cover data are prepared, the datasets are co-located at the same spatial grid. We specify the grid resolution for each community in the corresponding report. Consequently, the land-cover data are converted to a cost-inverse raster based on the speed-conservation values (SCVs) assigned to each feature type contained in the layer. SCVs represent the fraction of a maximum speed that could be achieved across the given land-cover type. For example, if the maximum travel speed is assumed to be on a road (SCV=1), the travel speed on any other land-cover surface would be some smaller percentage. For open water, we assume that no travel is possible and hence SCV is set to zero. Table 1 shows the typical land-cover types delineated for the community and their associated speed-conservation values (SCV). If additional land-cover types are necessary, their values are discussed for the particular case. We emphasize that in Scenarios 2 and 4, which model an evacuation to the boundary of the hazard zone by major roads, all SCVs not using roads are assumed to be zero.

Table 1. Relationships between 2011 Alaska National Land Cover Database (NLCD), PEAE land-cover classes, and speed-conservation values (SCVs)

NLCD description(s)	**PEAE land-cover types**	**Speed-conservation values (SCV)** *(proportion of maximum travel speed)*
Open water	Open water	0
*Not in NLCD as individual structures	Buildings	0
Barren land	Unconsolidated beach	0.5556
Emergent herbaceous wetlands	Wetlands	0.5556
Evergreen, mixed and deciduous forests	Heavy brush	0.6667
Grassland/herbaceous, dwarf shrub, shrub/ scrub	Light brush	0.8333
Open space, developed (low to high intensity)	Developed area	0.9091
*Not in NLCD as specific feature	Roads	1

Step 2

The path-distance tool uses elevation gradients between the neighboring cells and the cost-inverse raster derived in Step 1 and computes a cost distance from every cell in the study area to the boundary of the tsunami hazard zone (Scenarios 1 and 3) or to the nearest assembly area (Scenarios 2 and 4). Note that the elevation gradient depends on the spatial resolution of the DEM, and in areas near the abrupt cliffs some large values of the gradients may intrude onto the flat areas. This phenomena could cause instances of unrealistically high travel time in the vicinity of the sudden elevation change and need to be screened. Because the path-distance values represent an "effective" distance to safety and are by themselves meaningless until they are divided by the assumed travel speed, the screening process is completed in Step 3.

Step 3

The evacuation-time surface is calculated by dividing the path-distance surface by a travel or walking speed. In this report we set the base speed of the evacuee to be comparable to the “slow walk” speed option (0.91 m/s or 3 ft/s) in the PEAE settings. Wood and Schmidtlein (2012) note that a base travel speed of 1.1 m/s (3.6 ft/s) represents the 15th percentile of walking speeds of a mixed population and is the recommended speed for crosswalk walking speed standards in the United States (United States Department of Transportation, 2009). We chose to use the “slow walk” value to model the most conservative estimates of time to safety. This is a very

conservative speed and many residents should be able to evacuate twice as fast (1.52 m/s [5 ft/s] "fast walk", if not 1.79 m/s [5.9 ft/s] "slow run") as the modeled rate. Future reports might consider a variety of scenarios using varying walking speeds.

Because of a potential occurrence of the above-mentioned artifacts in the path-distance surface, we visually screen the computed travel-time maps for any unrealistically high travel times (Jones and others, 2014). In particular, we review the histograms of the travel time and eliminate the extreme outlier times. Refer to Jones and others (2014) for details regarding the determination of the maximum time value for the pedestrian to travel to a safe location.

Step 4

Once the evacuation-time surface is calculated, it is reclassified into an integer raster with 1-minute increment bands.

Step 5 (Optional)

If the hypothetical vertical evacuation structures, such as buildings or berms, are considered in the modeling study, we consider an additional assembly area at the location of the vertical evacuation structure, and consequently execute Steps 1–4 again.

MODEL VALIDATION

The spatial resolution of input data layers can significantly influence the accuracy of the calculated travel times, with the elevation resolution having a much more dramatic impact on modeled pedestrian travel times than land-cover resolution (Wood and Schmidtlein, 2012). To test the accuracy of the computed time maps, we perform a model verification study for each community considered. In particular, we compared the computed travel times to safety with actual walking times gathered during community site visits. Although it is not possible to walk every potential route to safety and match the modeled walking speed exactly, every effort was made to walk and accurately time the major routes, as well as collect data with a handheld GPS receiver. The model validation study and the route descriptions are provided in each community report.

SOURCES OF ERRORS AND UNCERTAINTIES

The modeling approach described in this report cannot exactly represent an actual evacuation; and, as with all evacuation models, the LCD approach cannot fully capture all aspects of individual behavior and mobility (Wood and Schmidtlein, 2012). Weather conditions, severe shaking, soil liquefaction, collapse of infrastructure, downed electrical wires, and the interaction of individuals during the evacuation will all influence evacuee movement. We employ a "slow walk" base travel speed of 0.91 m/s (3 ft/s) that is assumed to create the most conservative times to evacuation. At-risk populations in tsunami-prone areas will vary in their degree of mobility and their ability to travel long distances in short time periods. Actual conditions during an evacuation event could vary from those considered, so the accuracy cannot be guaranteed.

In analyzing the computed travel times, a reader should note that the LCD approach assumes that a pedestrian takes an optimal route to safety (Wood and Schmidtlein, 2012). However, some individuals less familiar with the area might take a less optimal route and will require a longer time to reach safety. Moreover, in case of emergency, some individuals might require some time to confirm imminent personal danger from the tsunami and possibly delay their evacuation. Therefore, quantitative assessments of evacuation times determined that the results from our method should only be considered guidelines to determining the evacuation potential of each community.

SUMMARY

In this report, we provide a brief review of the Pedestrian Evacuation Analyst Extension (PEAE) for ArcGIS (Jones and others, 2014) and steps required to compute pedestrian travel-time maps for selected Alaska coastal communities. We emphasize that high-resolution elevation data, detailed and accurate land cover, and up-to-date roads information are required to yield accurate travel-time maps.

ACKNOWLEDGMENTS

This project received support from the National Oceanic and Atmospheric Administration (NOAA) under Reimbursable Service Agreement ADN 952011 with the State of Alaska's Division of Homeland Security and Emergency Management (a division of the Department of Military and Veterans Affairs). Thoughtful reviews by Nathan Wood of the U.S. Geological Survey improved the report and maps.

References

Dunbar, P.K., and Weaver, C.S., 2008, U.S. states and territories national tsunami hazard assessment—Historical record and sources for waves: National Oceanic and Atmospheric Administration and U.S. Geological Survey, Technical Report, 59 p. http://nthmp.tsunami.gov/documents/Tsunami_Assessment_Final.pdf

Estabrook, C.H., Jacob, K.H., and Sykes, L.R., 1994, Body wave and surface wave analysis of large and great earthquakes along the eastern Aleutian arc, 1923–1993—Implications for future events: Journal of Geophysical Research, v. 99, no. B6, p. 11,643–11,662. doi:10.1029/93JB03124

Jin, Suming, Yang, Limin, Danielson, Patrick, Homer, Collin, Fry, Joyce, and Xian, George, 2013, A comprehensive change detection method for updating the National Land Cover Database to circa 2011: Remote Sensing of Environment, v. 132, p. 159–175. doi:10.1016/j.rse.2013.01.012

Johnson, J.M., and Satake, Kenji, 1993, Source parameters of the 1957 Aleutian earthquake from tsunami waveforms: Geophysical Research Letters, v. 20, no. 14, p. 1,487–1,490. doi:10.1029/93GL01217

Jones, J.M., Ng, P., and Wood, N.J., 2014, The pedestrian evacuation analyst—Geographic information systems software for modeling hazard evacuation potential: U.S. Geological Survey Techniques and Methods, book 11, chapter C9, 25 p. doi:10.3133/tm11C9

Kanamori, Hiroo, 1970, The Alaska earthquake of 1964—Radiation of long-period surface waves and source mechanism: Journal of Geophysical Research, v. 75, no. 26, p. 5,029–5,040.

Lopez, A.M., and Okal, E.A., 2006, A seismological reassessment of the source of the 1946 Aleutian 'tsunami' earthquake: Geophysical Journal International, v. 165, no. 3, p. 835–849. doi:10.1111/j.1365-246X.2006.02899.x

National Geophysical Data Center/World Data Service (NGDC/WDS), in progress, Global historical tsunami database at NGDC, 2100 BC to present [interactive map]: National Geophysical Data Center, NOAA. doi:10.7289/V5PN93H7

Nicolsky, D.J., Suleimani, E.N., Combellick, R.A., and Hansen, R.A., 2011, Tsunami inundation maps of Whittier and western Passage Canal, Alaska: Alaska Division of Geological & Geophysical Surveys Report of Investigation 2011-7, 65 p. doi:10.14509/23244

Nicolsky, D.J., Suleimani, E.N., Freymueller, J.T., and Koehler, R.D., 2015, Tsunami inundation maps of Fox Islands communities, including Dutch Harbor and Akutan, Alaska: Alaska Division of Geological & Geophysical Surveys Report of Investigation 2015-5, 67 p., 2 sheets, scale 1:12,500. http://doi.org/10.14509/29414

Nicolsky, D.J., Suleimani, E.N., Haeussler, P.J., Ryan, H.F., Koehler, R.D., Combellick, R.A., and Hansen, R.A., 2013, Tsunami inundation maps of Port Valdez, Alaska: Alaska Division of Geological & Geophysical Surveys Report of Investigation 2013-1, 77 p., 1 sheet, scale 1:12,500. doi:10.14509/25055

Nicolsky, D.J., Suleimani, E.N., and Koehler, R.D., 2014, Tsunami inundation maps of Cordova and Tatitlek, Alaska: Alaska Division of Geological & Geophysical Surveys Report of Investigation 2014-1, 49 p. doi:10.14509/27241

Suleimani, E.N., Nicolsky, D.J., and Koehler, R.D., 2013, Tsunami inundation maps of Sitka, Alaska: Alaska Division of Geological & Geophysical Surveys Report of Investigation 2013-3, 76 p., 1 sheet, scale 1:250,000. doi:10.14509/26671

Suleimani, E.N., Nicolsky, D.J., and Koehler, R.D., 2015, Tsunami inundation maps of Elfin Cove, Gustavus, and Hoonah, Alaska: Alaska Division of Geological & Geophysical Surveys Report of Investigation 2015-1, 79 p. doi:10.14509/29404

Suleimani, E.N., Nicolsky, D.J., West, D.A., Combellick, R.A., and Hansen, R.A., 2010, Tsunami inundation maps of Seward and northern Resurrection Bay, Alaska: Alaska Division of Geological & Geophysical Surveys Report of Investigation 2010-1, 47 p., 3 sheets, scale 1:12,500. doi:10.14509/21001

Wood, N.J., and Schmidtlein, M.C., 2012, Anisotropic path modeling to assess pedestrian-evacuation potential from Cascadia-related tsunamis in the U.S. Pacific Northwest: Natural Hazards, v. 62, no. 2, p. 275–300. doi:10.1007/s11069-011-9994-2

Wood, N.J., and Schmidtlein, M.C., 2013, Community variations in population exposure to near-field tsunami hazards as a function of pedestrian travel time to safety: Natural Hazards, v. 65, no. 3, p. 1,603–1,628. doi:10.1007/s11069-012-0434-8

Wood, N.J., and Peters, Jeff, 2015, Variations in population vulnerability to tectonic and landslide-related tsunami hazards in Alaska: Natural Hazards, v. 75, no. 2, p 1,811-1,831. doi:10.1007/s11069-014-1399-6

United States Department of Transportation, 2009, Manual on uniform traffic control devices for streets and highways: Federal Highway Administration, 816 p. http://mutcd.fhwa.dot.gov/

Wu, F.T., and Kanamori, Hiroo, 1973, Source mechanism of February 4, 1965, Rat Island earthquake: Journal of Geophysical Research, v. 78, no. 26, p. 6,082–6,092. doi:10.1029/JB078i026p06082

Yeh, H., Fiez, T., and Karon, J., 2009, A comprehensive tsunami simulator for Long Beach Peninsula, Phase-1—framework development final report: Tacoma, WA, State of Washington Military Department, Emergency Management Division, 27 p.